EPR and AM1 Study of the Structure of the Radical Anion of *β*-ionone

Alexander I. Kruppa, Tatyana V. Leshina, and Valery V. Konovalov[†]

Institute of Chemical Kinetics and Combustion, Novosibirsk, 630090, Russia

Lowell D. Kispert*

Chemistry Department, University of Alabama, Tuscaloosa, Alabama 35487-0336

Received: October 21, 1998; In Final Form: December 31, 1998

The structure of the radical anion of *β*-ionone has been investigated by EPR and AM1 molecular modeling methods as a part of a study to determine the structure and magnetic properties of intermediates of one-electron transfer reactions of carotenoids. Analysis of the temperature dependence of the EPR spectrum of the radical anion shows that the largest hyperfine coupling of 16 G previously assigned to the 7-H proton should be assigned to the 4-H proton in the axial orientation. The previous assignment failed to account for rate of the cyclohexene ring inversion. Comparing the resolved EPR spectra at various temperatures indicates that the coupling of 7-H proton equals ≈ 9.5 G. The structure of the radical anion predicted by AM1 molecular modeling is in agreement with this analysis. From the temperature dependence the rate of the cyclohexene ring inversion in the radical anion at room temperatures is approximately 6×10^7 s^{-1} with an activation energy of about 7 kcal/mol.

Introduction

Carotenoids have been investigated for many years because of their biological importance.[1,2] Several studies have been devoted to the investigation of carotenoid intermediates due to their role in photochemical[3] and electrochemical processes.[4] Except for the oxygen atom, the structure of *β*-ionone (**I**) is the same as C1 to C9 in the carotenoid *β*-carotene (Scheme 1).

The photochemical reactions of **I** have been investigated in detail under various experimental conditions,[5] and the influence of electron-donating and electron-accepting properties on the reaction outcome has been demonstrated.[6,7] But there are only a few studies that deal with the direct observation of its paramagnetic intermediates. Guzzo et al. were the first to detect the EPR spectrum of the electrochemically generated radical anion of **I** in tetrahydrofuran at −70 °C,[8] and suggested a 40° twist around the C6−C7 bond of the radical anion because this seemed to be the only structure that could explain the observed spin density distribution.[9] Other investigators did not agree with this interpretation of the radical anion structure.[10] Quantum chemical modeling and NMR investigation for long-chain carotenoids predict only small or no twisting.[11] Recently we were interested in studying one-electron transfer reactions of carotenoids by spin chemistry techniques (CIDNP and CIDEP).[12] Since the structure and magnetic properties of the probable intermediates are of importance for interpretation of the spin chemistry, experimental data are necessary to study these intermediates.

The present study is devoted to the investigation by EPR and AM1 molecular modeling techniques of the structure and magnetic properties of the radical anion of **I**.

Experimental Section

Instrumental. Cyclic voltammograms (CV) were recorded with a 1 mm disk Pt electrode by using a BAS-100A electrochemical analyzer. EPR experiments were carried out with an electrochemical flat cell using a Varian E-12 EPR spectrometer. Both the working and auxiliary electrodes were platinum wires, and the reference electrode was a silver wire (diameter 75 μm). The area of the working electrode inside the EPR cavity was about 1 cm^2. EPR spectra were recorded under bulk electrolysis (BE) conditions by using the BAS-100A. The potential applied to the EPR cell was periodically controlled by CV scans with the flat cell directly in the EPR cavity. The potential for BE exceeded the potential of the first reduction wave of *β*-ionone by 100 mV. The magnetic field was measured with a Bruker EPR 035M gaussmeter, and the microwave frequency was measured with a Model HP 5245L frequency counter. The AM1 semiempirical quantum chemical method (HyperChem 4 software) was used for the geometry optimization of the radical anion and to estimate the spin density distribution. Both restricted (RHF) and unrestricted (UHF) Hartree−Fock approximations were used. Computer simulation of the EPR spectra was made by taking second-order effects into account.

SCHEME 1

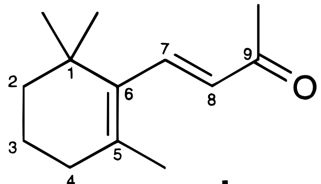

I

Chemicals. Acetonitrile (ACN) (Aldrich, 99.8%, water < 0.005%) and dimethylformamide (DMF) (Burdick and Jackson, HPLC grade, water < 0.009%) were used without additional purification and stored in unopened (Aldrich Sure/Seal cap) bottles under Ar atmosphere. Tetrahydrofuran (THF) (Aldrich, 99.5%, water <0.02%) was stored in a glass flask with small amounts of anthracene and potassium metal. For the EPR experiments only freshly distilled THF was used. The tetrabu-

---

* Author to whom correspondence should be addressed.

[†] Present address: Department of Chemistry, University of Alabama.

10.1021/jp984111k CCC: $18.00

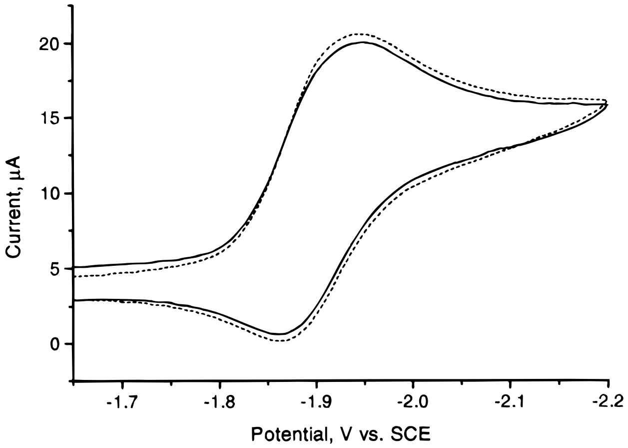

Figure 1. CV of solution of the 5 mM β-ionone solution in ACN (0.1 M TBAHFP) recorded at different scan rates, 100 mV/s (solid line) and 500 mV/s (dashed line). $T = 295$ K.

tylammonium hexafluorophosphate (TBAHFP) and tetrabutylammonium perchlorate (TBAPC) (both Fluka, polarographic grade) were used as supplied and stored in the drybox under nitrogen. β-Ionone (Aldrich, 96%) was purified by silica gel column chromatography using a 10:1 (v/v) mixture of hexane and ethyl acetate as eluent.

Sample Preparation. The supporting electrolyte solution, 0.1 M TBAHFP(TBAPC), was prepared in a drybox. Electrolyte and β-ionone solutions were transferred by syringe to a septum-stoppered volumetric flask. After 20 min bubbling by Ar, the solution was transferred by syringe to the EPR electrolytic cell and again deaerated by argon bubbling for 10 min.

The concentration of β-ionone used for CV and EPR measurements was 5 mM.

Results and Discussions

The CVs of β-ionone solutions in ACN (see Figure 1) show reversible reduction wave behavior with $E_{1/2}^{\text{red}} = -1.89$ V vs SCE. This value is close to the previously reported value of -1.85 V vs SCE (ACN, 0.1 M TBAPC, 20 °C).[6] From these data it is assumed that the radical anion of **I** is quite stable at room temperature.

The experimental EPR spectrum of the radical anion of **I** in ACN at 20 °C is shown in Figure 2a. The g-factor of the radical anion calculated from the spectrum is 2.0036 ± 0.0001, which coincides with the literature data.[10] The spectral width has the same value (74 G) as reported previously.[8,10] The best simulated first derivative of the EPR spectrum is shown in Figure 2b. As can be seen by comparing the experimental and simulated data, the spectrum is well described in terms of three different groups of protons: two different protons and six equivalent protons. The values of hyperfine coupling constants and g-factors obtained for various solvents and supporting electrolytes are summarized in Table 1.

In a previously reported study of β-ionone reduction by solvated electrons in liquid ammonia at 200 K,[10] the EPR spectrum was assigned to $g = 2.0036$ and the following set of HFC values: 1H(7-H): 16.23 G; 1H(4-H): 9.79 G; 1H(4-H): 8.41 G; 3H(5-CH_3): 6.48 G; 3H(9-CH_3): 6.48 G; 1H(8-H): $<$ 0.83 G. For the β-ionone radical anion generated electrochemically in THF at 200 K, the couplings were assigned as 1H(7-H): 15.9 G; 2H(4-H): 9.5 G; 3H(CH_3): 6.5 G; 3H(CH_3): 6.5 G; 1H(8-H): $<$ 1.6 G.[9]

These data were obtained at low temperature and are inconsistent with our assignment at room temperature. This difference between the room- and low-temperature spectra may arise from the temperature dependence of the EPR spectra. The fundamental difference is the absence of a coupling of about 16 G and a second coupling of about 9.5 G at room temperature. Under our experimental conditions the spectrum clearly demonstrates a single coupling with a separation equal to the sum of these hyperfine couplings. This situation resembles the well-known vinyl radical problem for which all the components of the EPR spectrum are observable only at liquid helium temperature.[13] With increasing temperature the inner components of the spectrum fully disappear due to the vinyl radical conformational transitions.[14]

The previously suggested assignment was explained by the existence of a rigid twist around the C6$-$C7 bond of the β-ionone radical anion structure for which the largest HFC was assigned to 7-H.[9] This large coupling at 7-H was attributed to the β-effect between C6-p_Z and 7-H proton that produces a coupling larger than those expected for the planar C5$-$C6$-$C7$-$C8 structure. We propose that this assignment does not correspond to a physically reasonable radical anion structure.[10]

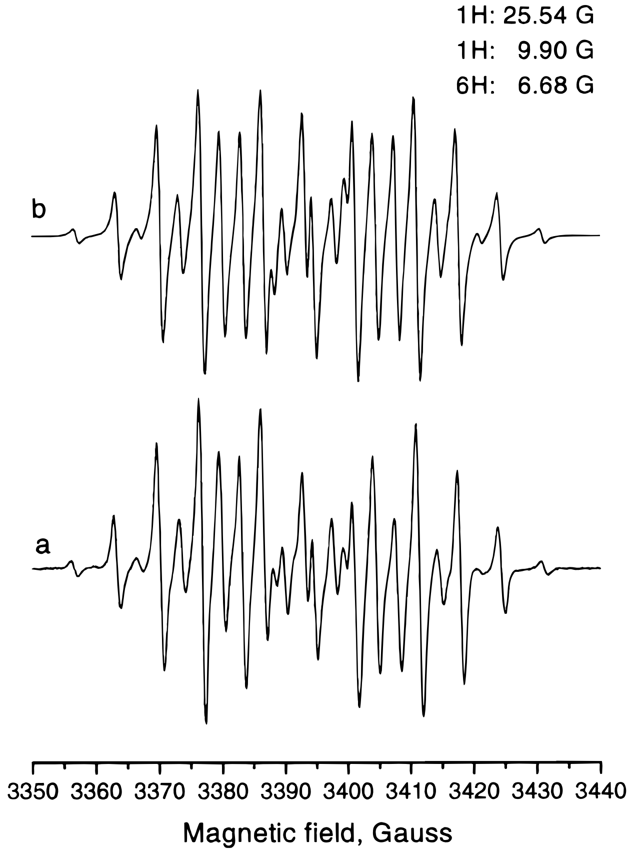

Figure 2. (a) EPR spectrum of the electrochemically generated radical anion of β-ionone. β-Ionone (5 mM) in ACN (0.1 M TBAHFP). $\nu = 9.5148$ GHz, microwave power 2 mW, modulation amplitude 0.5 G, $T = 295$ K; (b) Simulated EPR spectrum of radical anion in ACN.

TABLE 1: Experimental Hyperfine Constants and g-Factors in Different Solvents and Supporting Electrolytes

solvent	supporting electrolyte (0.1 M)	HFC,[a] Gauss 1H	1H	6H	g-factor ($\pm$0.0001)
ACN	TBAHFP	25.54	9.90	6.68	2.0036
DMF	TBAHFP	25.18	9.70	6.24	2.0036
THF	TBAHFP	24.80	9.42	6.41	2.0036
THF	TBAPC	24.80	9.42	6.41	2.0036

[a] Obtained from the best simulation of experimental spectra.

TABLE 2: Optimized AM1/UHF Geometry of the β-Ionone Radical Anion

Structure	Internal coordinates						
	a	R_{ab}	*b*	∠*abc*	*c*	∠*abcd*	*d*
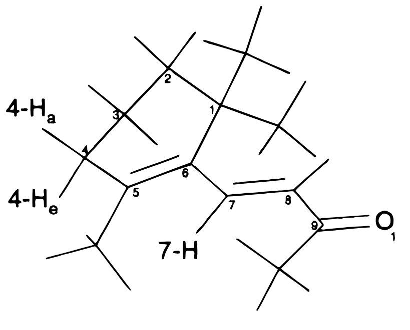 **i**	C5	1.477	C4				
	C6	1.389	C5	124.4	C4		
	C7	1.414	C6	119.5	C5	-180.0	C4
	C8	1.384	C7	130.4	C6	166.9	C5
	C9	1.424	C8	124.6	C7	177.8	C6
	O1	1.263	C9	123.0	C8	177.8	C7
	$4H_a$	1.128	C4	109.6	C5	-103.9	C6
	$4H_e$	1.126	C4	110.2	C5	139.8	C6
	7H	1.108	C7	114.7	C6	-11.6	C5
ΔH_0 = -66.3 kcal/mol[a]							
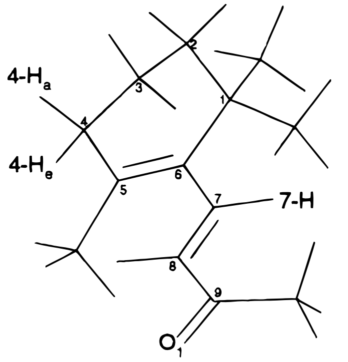 **ii**	C5	1.481	C4				
	C6	1.381	C5	123.5	C4		
	C7	1.413	C6	125.9	C5	172.8	C4
	C8	1.384	C7	129.1	C6	-19.1	C5
	C9	1.422	C8	124.6	C7	176.1	C6
	O1	1.264	C9	123.3	C8	177.0	C7
	$4H_a$	1.126	C4	109.2	C5	-98.5	C6
	$4H_e$	1.125	C4	110.4	C5	145.2	C6
	7H	1.107	C7	115.1	C6	161.4	C5
ΔH_0 = -66.0 kcal/mol[a]							

[a] Heat of formation by means AM1.

AM1 molecular modeling of the β-ionone radical anion predicts the existence of two minimum energy conformations. The calculated structures and their parameters are presented in Table 2. Data from Table 2 show that the optimized structures of the radical anion exist as a nearly planar conjugated system C7–C8–C9–O1 (dihedral angle is 177.0°). The C5–C6 double bond of the cyclohexene fragment is slightly twisted from the planar conjugated system (13° and 19° for minimum energy structures, see Table 2). The calculated dependence of the radical anion heat of formation ΔH_0 on the torsion angle between the planes of C5–C6 and C7–C8 double bonds is shown in Figure 3. A low-energy torsional barrier is not in agreement with the proposed rigid structure. Because AM1 is one of most accurate semiempirical quantum chemical method available, one can assume that the real radical anion structure has an average torsion angle about 15° which simultaneously oscillates in the range of ±45° from the average value at the temperature under study.

AM1 optimized structures show that the 4-H protons are magnetically nonequivalent because they have different orientations with respect to the C5-p_Z orbital. For the structure **i**, the dihedral angles Θ between 4-CH bonds and C5-p_Z orbital are about 14° and −50° for axial and equatorial orientation, respectively (9° and −55° for structure **ii**). The ratio of the coupling for the 4-H protons can be estimated as a ratio of squared cosines of Θ.[15] This gives $\mathbf{a}(4\text{-H}_a)/\mathbf{a}(4\text{-H}_e) = 1.90(2.32)$. Usually the AM1 method cannot predict accurate spin density distribution, but it has been useful to predict relative HFC values. Thus the coupling for the 4-H protons obtained by UHF/AM1 calculations for optimized structures are 16.5 and 6.8 G (for both structures), in agreement with simple estimates.

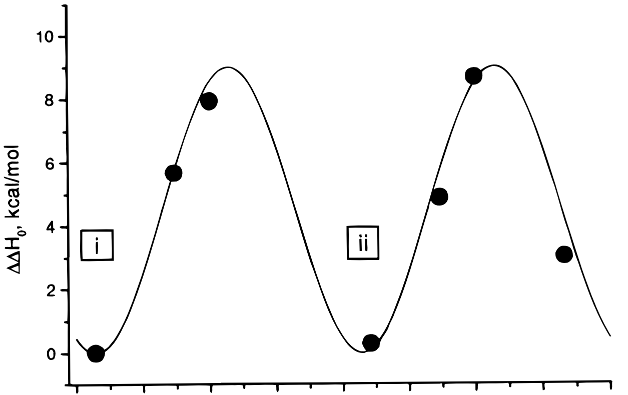

Figure 3. AM1 calculated dependence of variation of the heat of formation of the β-ionone radical anion on the torsion angle between the C5–C6 and C7–C8 double bonds; **i** and **ii** correspond to minimum energy structures from Table 2.

The presence of these magnetically nonequivalent protons in the cyclohexene fragment can explain the observed temperature effect in the EPR spectra because ring inversion causes mutual reorientation of the 4-H protons (Scheme 2):

The existence of nonequal splitting from these protons at low temperature implies that in the radical anion the cyclohexene ring inversion process is not rapid enough to average the

SCHEME 2

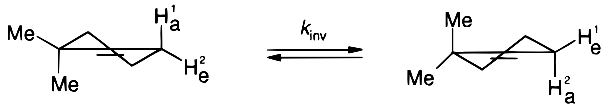

coupling of the 4-H protons. Ring inversion has been very extensively investigated for many years by NMR.[16] It was determined that the activation energy (E_a) for ring inversion of the cyclohexene is about 5 kcal/mol.[16] It was also found that substitution of CH_2−protons by methyl groups increases the E_a of inversion by 2−3 kcal/mol.[17] Thus it is reasonable to estimate E_a as 7−8 kcal/mol. This value leads to slow ring inversion at low temperature and strong temperature dependence on the ring inversion rate.

The above lead us to reassign the coupling of the β-ionone radical anion as:

$$1H(7\text{-}H):\ 9.5-9.9\ G$$

$$6H(5\text{-}CH_3 \text{ and } 9\text{-}CH_3):\ 6.4-6.7\ G$$

$$1H(4\text{-}H_a):\ \approx 15.5\ G$$

$$1H(4\text{-}H_e):\ \approx 9.5\ G$$

$$1H(8\text{-}H):\ < 0.8\ G, \text{ estimated from EPR line width.}$$

This reassignment allows us to present an explanation for the observed temperature effect for the β-ionone radical anion EPR spectrum.

The nuclear spin states for the 4-H protons form four sub-ensembles: $\alpha_a\alpha_e$, $\alpha_a\beta_e$, $\beta_a\alpha_e$, and $\beta_a\beta_e$. It is obvious that ring inversion results in exchange between $\alpha_a\beta_e$ and $\beta_a\alpha_e$. From the theory of magnetic resonance it is known that lines corresponding to these nuclear sub-ensembles can depend on the exchange rate.[18] First, the rate of ring inversion is slow in comparison with the lifetime predicted by the native line width. In this case all lines of EPR spectra will be observable and the EPR spectrum will have well-resolved hyperfine splitting as is observed at low temperature. When the ring inversion rate increases with temperature, then the EPR components for $\alpha_a\beta_e$ and $\beta_a\alpha_e$ will be broadened proportional to the increase in the exchange rate.[18] When the temperature becomes high enough, the inner components collapse to a single broadened component, resulting in a doublet of septets structure from the splitting by the 7-H and two methyl groups. This situation is well described in the literature and correlates with a fast exchange rate.[18] Because of the exchange, the outer sharp components ($\alpha_a\alpha_e$ and $\beta_a\beta_e$) can mask the inner broadened components of EPR spectra. For this case the absorption EPR spectrum (the integral of the original first derivative) may be more informative. Figure 4 presents the simulated absorption EPR spectrum (Figure 4a corresponds to Figure 2b) and experimental spectrum (Figure 4d corresponds to Figure 2a). Note that the simulation was made for data presented in Table 2 and describes only the outer components of the EPR spectrum. As seen from Figure 4, the EPR experimental absorption spectrum (Figure 4d) differs from the simulated one (Figure 4a). The experimental spectrum clearly shows that in addition to well-resolved sharp lines from the outer components, there is an absorption from the inner components. The resulting spectrum may be described as a superposition of the spectrum of the outer components (Figure 4a) and the broadening coalescence of the inner components (Figure 4b). The superposition spectrum is presented in Figure 4c and demonstrates excellent agreement with the experimental spectrum (Figure 4d). The best simulation of the EPR spectrum with the full set of protons and their couplings was obtained with a line width of 2.2 G for the inner component. Because of the overlapping lines in the center of the EPR spectrum, it is difficult to study the inversion rate quantitatively. Nevertheless, from the simulated line width for the inner component, it is possible to evaluate the cyclohexene ring inversion rate at room temperature. Since the exchange mixes only two spin states ($\alpha_a\beta_e$ and $\beta_a\alpha_e$) and other nuclei do not change their spin projection, the individual line width of inner components ($1/T_2$) can be described in terms of a simple two-line exchange model. For the fast exchange limit, the ring inversion rate constant may be found from the equation[14,18]

$$\frac{1}{T_2} = \frac{1}{T_2^{\,0}} + \frac{(\omega_a + \omega_b)^2}{8k_{inv}}$$

where $1/T_2^{\,0}$, the line width in the absence of exchange processes, can be estimated from the experimental line width of outer components (0.8 G); the initial coupling between lines is equal to the difference of the 4-H_a and 4-H_e couplings (about 6 G). The average obtained in this manner is $6 \times 10^7\ s^{-1}$. Estimation of the activation energy by the Arrhenius equation (for usual preexponential factor value $10^{13}\ s^{-1}$) gives 7.4 kcal/mol which is close to that cited above from NMR measurements.

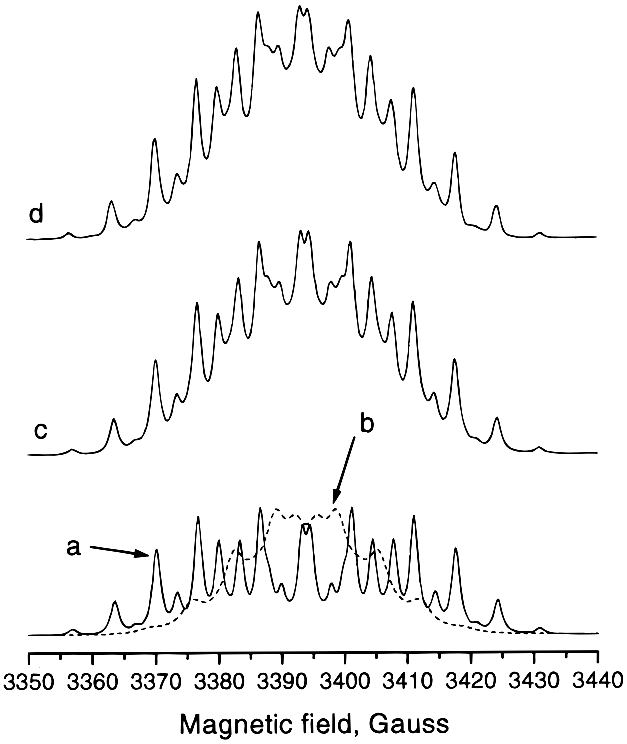

Figure 4. (a) EPR simulated spectra for outer (solid line) and (b) inner (dashed line) components; (c) superposition of inner and outer components; (d) experimental EPR spectrum.

Thus we conclude that the previous assignment of hyperfine coupling in the β-ionone radical anion was not correct. The largest coupling of 16 G should be assigned to the 4-H proton in the axial conformation. The 7-H coupling cannot be averaged during the conformational transitions of the radical anion. By comparing the resolved EPR spectra at various temperatures the coupling has a value of about 9.5 G. The structure of the radical anion predicted by AM1 molecular modeling is in agreement with experimental data. For the radical anion under study, the rate of the cyclohexene ring inversion at room temperatures is approximately 6×10^7 s^{-1}. The activation energy of this process is about 7 kcal/mol.

Acknowledgment. This work was supported by U.S. Civilian Research and Development Foundation (CRDF) under Grant RC1-175. A. I. Kruppa thanks *Young Investigator Research Opportunities of CRDF Collaborations Program* of CRDF and the Russian Foundation for Basic Research (RFBR) for support. Laboratory supplies and equipment were supported by the Division of Chemical Sciences, Office of the Basic Energy Sciences, Office of Energy Research of the U.S. Department of Energy under Grant DE-F602-86ER13465. The authors thank Dr. Tatyana Konovalova and Dr. Elli Hand for helpful discussions during manuscript preparation.

References and Notes

(1) Krinsky, N. I.; Mathews-Roth, M. M.; Taylor, R. F. *Carotenoids: Chemistry and Biology*; Plenum: New York, 1990.

(2) Goodwin, T. V. *The Biochemistry of Carotenoids*, 2nd ed.; Chapman and Hall: London, 1980; Volumes 1 and 2.

(3) Truscott, T. G. *J. Photochem. Photobiol. B: Biol.* **1990**, *6*, 359.

(4) Mairanovsky, V. G.; Engovatov, A. A.; Ioffe, T. N.; Samokhvalov, G. I. *J. Electroanal. Chem*. **1975**, *66*, 123. Jeevarajan, A. S.; Khaled, M.; Kispert, L. D. *J. Phys. Chem*. **1994**, *98*, 7777.

(5) van Wageningen, A.; Cerfontain, H.; Geenevasen, J. A. J. *J. Chem. Soc., Perkin 2* **1975**, 1283. Cerfontain, H.; Geenevasen, J. A. J. *Tetrahedron* **1980**, *37*, 1571.

(6) Cerfontain, H.; Geenevasen, J. A. J.; van Noort, P. C. M. *J. Chem. Soc., Perkin Trans. 2* **1980**, 1057.

(7) Mallik, B.; Jain, K. M.; Misra, T. N. *Biochem. J*. **1980**, *189*, 547.

(8) Harbour, J.; Guzzo, A. V. *Mol. Phys*. **1971**, *20*, 565.

(9) Harbour, J.; Guzzo, A. V. *Mol. Phys*. **1972**, *23*, 151.

(10) Elson, I. H.; Kemp, T. J.; Greatorex, D.; Jenkins, D. B. *J. Chem. Soc., Faraday Trans. 2* **1973**, *69*, 665.

(11) Hand, E. S.; Belmore, K. A.; Kispert, L. D. *J. Chem. Soc., Perkin Trans. 2* **1993**, 659. Hashimoto, H.; Miki, Y.; Kuki, M.; Shimamura, T.; Utsumi, H.; Koyama, Y. *J. Am. Chem. Soc*. **1993**, *115*, 9216. Jeevarajan, A. S.; Wei, C.; Kispert, L. D. *J. Chem. Soc., Perkin Trans. 2* **1994**, 861. *Carotenoids*; Isler, O., Ed.; Birkhäuser Verlag: Basel, 1971; Chapter 4.

(12) Polyakov, N. E.; Bashurova, V. S.; Schastnev, P. V.; Leshina, T. V. *J. Photochem. Photobiol. A: Chem*. **1997**, *107*, 55. Jeevarajan, A. S.; Khaled, M.; Forbes, M. D. E.; Kispert, L. D. *Zeit. Phys. Chem*. **1993**, *182*, 51.

(13) Cochan, E. L.; Adrian, F. J.; Bowers, V. A. *J. Chem. Phys*. **1963**, *40*, 213.

(14) This phenomenon is well discussed in EPR monographs; see, for example, Wertz, J. E.; Bolton, J. R. *Electron Spin Resonance*, 2nd ed.; Chapman and Hall: New York, 1986; Chapter 9.

(15) It is a well-known hyperconjugation mechanism of HFC; see, for example, Ayscough, P. B. *Electron Spin Resonance in Chemistry*, 1st ed.; Methuen: London, 1967; Chapter 3.

(16) See, for example, Fergusson, L. N. *Organic Molecular Structure*; Willard Grant: Boston, 1975; Chapter 18.

(17) Glaeson, G.; Androes, G. M.; Calvin, M. *J. Am. Chem. Soc*. **1961**, 83, 4357. Johnson, Ch. S., Jr. In *Advances in Magnetic Resonance*, Vol. 1; Waugh, J. S., Ed.; Academic Press: New York, 1965.

(18) See, for example, Carrington, A.; McLachlan, A. D. *Introduction to Magnetic Resonance*; Harper and Row: New York, 1967; Chapter 12.